Computational Fluid Dynamics Modeling of Cathodic Arc Jet

Anton Ronis* and Igal Kronhaus†

Faculty of Aerospace Engineering, Technion, Haifa, 3200003, Israel

In this paper a computational fluid dynamic (CFD) model is developed. A comparison with measurement data is made using spatial distribution of flow parameters as well as a *Taylor-Sedov* blast wave model analysis. The numerical solution is carried out using a modified `OpenFOAM` open source toolbox solver, `forcedIcoFoam` − a pressure based solver modified to include an external acceleration field acting on the flow. The flow properties − pressure and velocity qualitatively analyzed in different periods of simulation time. The pressure front position and static values, caused by the jet expansion with respect to time, are sampled and compared to the results obtained from experiment and the *Taylor-Sedov* blast model. The CFD jet model of the CAJ predicts well the observed phenomenons from experiments − *i.e.* forming of an initial cylindrical expansion zone at $1\ \mu s$, steady conditions in the jet area after around $t = 100\ \mu s$, and compatibility with the *Taylor-Sedov* blast model pressure front position and velocity, with respect to time and distance, respectively.

I.   Introduction

Active manipulation of flows is an important area of aeronautical research [1]. These devices or actuators promise benefits such as reduction of drag by delaying and/or eliminating separation zones [2]. Several examples of flow-control devices include: bumps, vanes (vortex generators), synthetic jets, bleed/suction and plasma actuators.

In contrary to other actuators, plasma actuators can operate on the flow by three different mechanisms [3]: momentum, shock and chemical effects. Momentum effects induce near surface flow velocities. Shock effects induce very high local gas pressure and temperature which creates gradients in the background air. Chemical effects introduce new species, such as ions, electrons, excited particles into the flow field. The most studied plasma actuator configuration is the dielectric barrier discharge (DBD) which is capable of inducing up to $\sim 10\ m/s$ flows [3–6], too low to be effective at high subsonic regimes.

In a recent study [7], cathodic arcs operating at atmospheric pressure environment were shown to produce fast jets of gas. This so called cathodic arc jet induce a local flow field velocities of $\geq 100\ m/s$ (see Fig. 1). The jet direction was shown to be controlled by the application of an external magnetic field. Subsequent experiments [8] conducted at different discharge currents suggested the development of a phenomenological model relating the cathode and background gas properties to the observed CAJ. The results suggest the possible use of a CAJ as a flow-control device for external subsonic flows [9].

---

*Graduate Student. E-mail: ro@tx.technion.ac.il

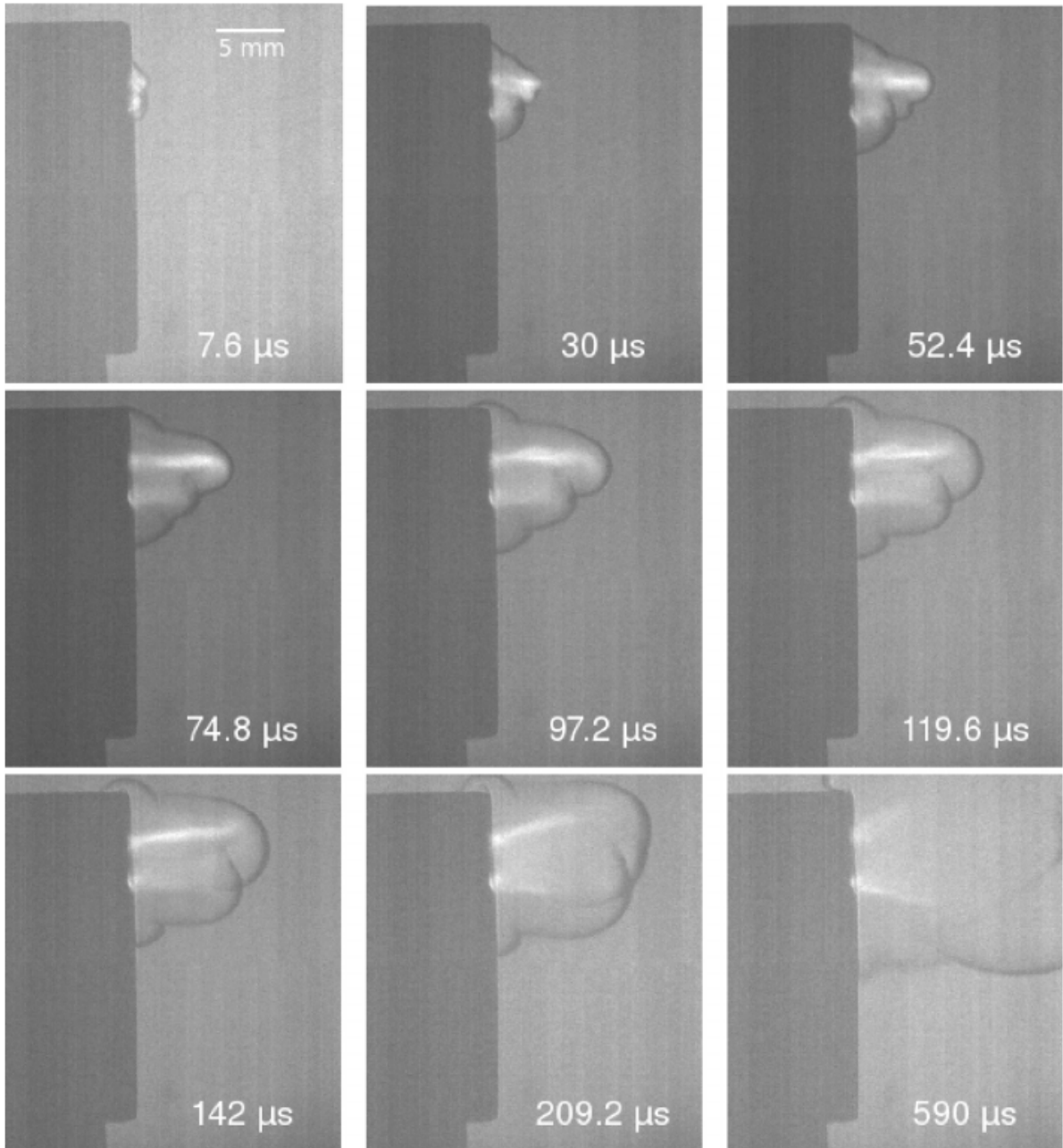†Assistant Professor. E-mail: kronhaus@technion.ac.il

Figure 1: Schlieren images of the cathodic arc jet in air. The luminous plasma shows white. The time is counted from the moment of ignition. Reproduced from [7].

II. Physical Model

Observing Fig. 1, we can divide the formation of a CAJ to two subsequent events:

1. Plasma formation in a bounded region

2. CAJ plume expansion towards the background gas

In the first event a small yet energized volume of plasma particles is generated. This shock boundary is formed in 1 μs for the given background pressure [10] and is bounded by a boundary radius which is related to the cathode parameters, discharge current and the background gas. The properties of this boundary radius are discussed in Subsection A.

Subsequently, the second event begins with an expansion of the energized volume generated at the discharge core. This expansion is followed by the formation of a jet caused by a momentum and energy transfer of the plasma particles to the gas. It is seen that after the initial boundary expansion certain *steady-state* conditions are met in the jet plume region. The initial expansion and resultant gas jet are discussed in Subsection B.

A. Plasma-Gas Boundary Radius

The force exerted on the plasma particles can be written as:

$$F_i \;=\; \frac{M_i V_i f}{Ze} I_d \tag{1}$$

Where M_i is the ion mass, V_i is the ion velocity, f is the ion current fraction, Z is the charge state, I_d is the current magnitude and e is the electron charge.

Constraining an equilibrium of forces between the plasma and gas we can use (1) to express the area, A, for a given pressure, p, for which an equilibrium is achieved:

$$F_g \;=\; F_i \tag{2}$$

$$pA \;=\; \frac{M_i V_i f}{Ze} I_d \tag{3}$$

$$A \;=\; \frac{M_i V_i f}{Ze} \frac{1}{p} I_d \tag{4}$$

Assuming cylindrical distribution of the gas pressure on the plasma, i.e $A = \pi r^2$, the following expression is obtained for the radius, r:

$$r \;=\; \mathcal{C}\sqrt{I_d} \tag{5}$$

Where $\mathcal{C} = \sqrt{\frac{1}{\pi} \frac{M_i V_i f}{Ze} \frac{1}{p}}$ is a constant defined by the cathode and experimental parameters. This allows us to relate the boundary radius r to the discharge current, I_d, thus resulting in a simplified relation between the two, for a given set of cathode parameters. By using known cathodic arc parameters for Cu ion in (5): $p = 101 \times 10^3$ Pa, ion mass $M_i = 1.055 \times 10^{-25}$ kg, ion velocity $V_i = 12.5 \times 10^3$ m/s, ion current fraction $f = 0.08$, charge state $Z = 1.8$ and I_d values measured in previous experiments [7,8] we can calculate the resultant boundary radius, r. Results for the given parameters are shown in Table 1.

Table 1: Calculated CAJ boundary radius

Parameter	Value	
p	101×10^3 Pa	
M_i	1.055×10^{-25} kg	
V_i	12.5×10^3 m/s	
f	0.08	
Z	1.8	
I_d	230 A	40 A
r	0.5 mm	0.2 mm

B. CAJ Plume Expansion Region

The preliminary effect of the high energized concentration of plasma can be modeled [7] as a disturbed expansion, corresponding with *Taylor-Sedov* blast wave model [11, 12]:

$$r^5 t^{-2} \quad = \quad \text{constant} \tag{6}$$

This expansion is measured to begin with a sonic velocity of ≈ 500 m/s [8], quickly decaying towards ≈ 50 m/s [7, 9] at ≈ 10 mm as visualized in Fig. 1.

Following the blast expansion is the formation of jet generated at the plasma-gas boundary. This jet is assumed to follow the initial blast expansion velocities close to the boundary while decreasing in velocity with the increase of distance from the boundary. The results summarized in Table 1 showcase that an equilibrium is achieved for distances of less than 1 mm. We can therefore assume that for farther regions (distances above 1 mm) a decay in the plasma density occurs – which corresponds to a loss of plasma energy. Assuming a conservation of energy in the plasma-gas spherical region, we can thus expect an increase in the gas' energy, in turn.

We note two main contributors to the generation of the jet inside the CAJ plume expansion zone: thermal – corresponding to heating the gas thus creating an expanding jet; momentum – corresponding to momentum transfer from the plasma particles and the gas by elastic collisions. As the jet is formed in a relatively small time-scale, we assume that the larger contributions comes from the momentum transfer due to the typical gas heat dissipation time constants [8].

Assuming steady state conditions at the boundary, we can express the exerted force on the gas with respect to velocity as:

$$F_g \quad = \quad \dot{m} V_g \tag{7}$$

Substituting the mass flux $\dot{m}$ for $\rho V_g A_o$ – where A_o represents a circular cross section through which the jet flows and ρ is the fluid density, yields:

$$F_g \quad = \quad \rho V_g^2 A_o \tag{8}$$

However, we know that the boundary radius defined by an equivalence between the flow's pressure field an the plasma's force. Comparing the former with (8) thus yields:

$$pA \;=\; \rho V_g^2 A_o \tag{9}$$

Substituting the areas A and A_o with the relevant expressions involving the boundary radius, r results in:

$$p \cdot \pi r^2 \;=\; \rho V_g^2 \cdot \pi r^2 \tag{10}$$

$$\frac{p}{\rho} \;=\; \frac{V_g^2}{2} \tag{11}$$

Using the state equation for an ideal gas, we get:

$$T \;=\; \frac{V_g^2}{R} \tag{12}$$

Where T is the temperature and R is the specific gas constant. (12) relates the gas temperature to the jet velocity. We can therefore express the Mach number at the boundary, as:

$$M \;=\; \frac{V_g}{a} \tag{13}$$

$$=\; \frac{\sqrt{RT}}{\sqrt{\gamma RT}} \tag{14}$$

$$=\; \sqrt{\frac{1}{\gamma}} \tag{15}$$

For most cases $\gamma \geq 1$, where specifically for ideal air $\gamma = 1.4$ – We can therefore conclude that the boundary Mach has high subsonic values.

III.   Numerical Model

The numerical approach is based on the assumption that the CAJ effect on the background gas can be simulated by an application of acceleration field which causes the gas to reach the velocities obtained in the [7]. Therefore the jet simulation corresponds to a hot gas expansion at a subsonic speed.

The numerical solution is carried out using a modified `OpenFOAM` [13] open source toolbox solver, based on the `icoFoam` solver. The `icoFoam` is a pressure based solver for transient incompressible flows which was modified to include an external force field acting on the flow.

The numerical domain consists of 250×400 grid points representing a 10 mm $\times$ 20 mm dimensioned physical domain.

We simulate the plasma-gas interaction by assuming a constant acceleration field just beneath the CAJ expansion plume region. The field properties are defined by the cathode spot and background gas parameters, as described in Section II, Subsection A. For the
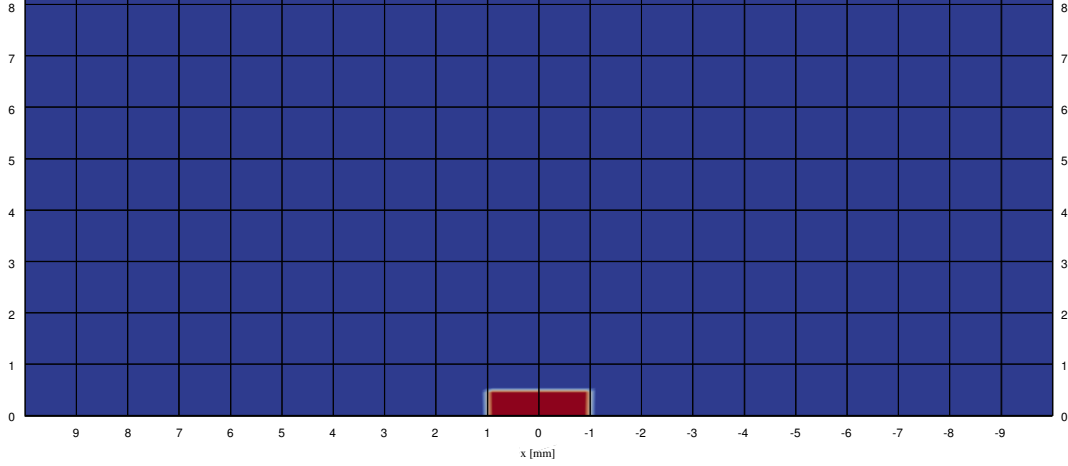
Figure 2: Force field representation in the numerical domain

observed parameters representing the experiment [7] of Fig. 1, the field was placed at $y < 0.5$ mm at a width of $r = 1$ mm (Fig. 2), centered around $x = 0$ mm. This corresponds to a discharge current of around 230 A.

Following measurement data [8], the acceleration field is adjusted to yield a velocity of 500 m/s. It is assumed that the discharge current affects the observed initial CAJ expansion velocity location, yet not the value itself, which in turn defined by the background gas properties [7–9]. The gas is assumed to be motionless, atmospheric at a room temperature. The added momentum resulted from the acceleration field is translated to an expansion of the gas in the form of a jet.

The simulation is executed at a modified time step constraining a Courant number, $\mathcal{C} \leq 0.1$, for a total simulation time of $t = 150\ \mu s$.

IV.   Results & Discussion

Running the simulation for $t = 150\ \mu s$ results in a velocity and pressure fields, as illustrated in Fig. 3a and Fig. 3b, respectively. The figures are sampled for the numerical domain region corresponding with the CAJ plume expansion region, i.e $y > 1$mm.

The simulation is sampled at the force field boundary which relates to the beginning of the CAJ plume expansion region $y = 1$mm at a width of $r = 0.5$mm, for both velocity and pressure in Table 2.

Table 2: Data sampled from simulation at equilibrium of forces, $t = 150\ \mu s$

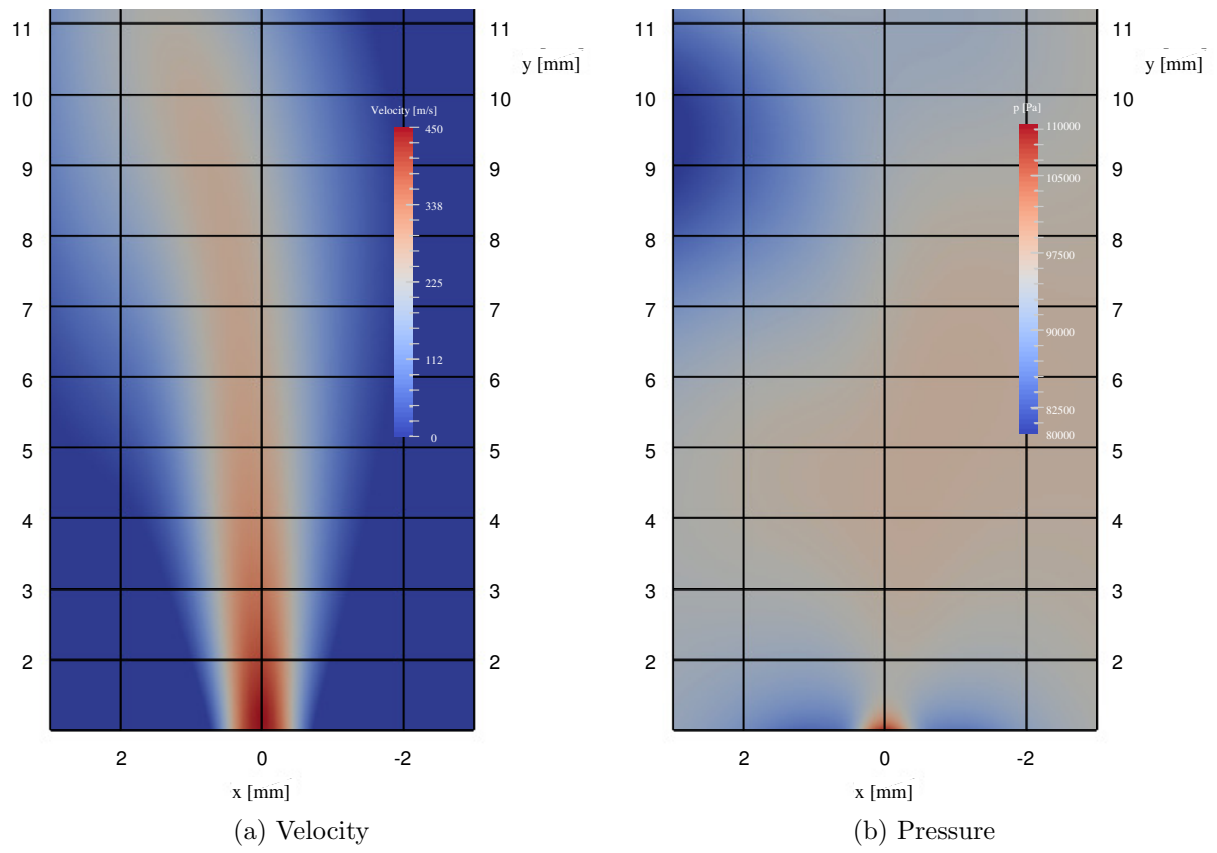|	$V_y[m/s]$	$p[Pa]$
Average	235	$102 \cdot 10^3$
Max	257	$10 \cdot 10^3$
Min	180	$98 \cdot 10^3$
σ	22	$2 \cdot 10^3$

Figure 3: (a) Velocity field, $t = 150 \ \mu s$; (b) Pressure field, $t = 150 \ \mu s$

References

[1] Gad-el-Hak, M., *Flow Control: Passive, active and reactive flow management*, Cambridge University Press, 2000.

[2] Simpson, R. L., "Turbulent boundary-layer separation," *Annual Review of Fluid Mechanics*, Vol. 21, No. 1, 1989, pp. 205–232.

[3] Ying-Hong, L., Yun, W., Hui-Min, S., Hua, L., and Min, J., "Plasma Flow Control," *Aeronautics and Astronautics*, edited by M. Mulder, 2011.

[4] Kok, J. C., Catalano, P., Kourtzanidis, K., Rogier, F., and Unfer, T., "Coupling of CFD with advanced plasma models," *ERCOFTAC Bulletin*, Vol. 94, 2013, pp. 29–34.

[5] Whalley, R., Debien, A., Podlinski, J., Jukes, T., K.S. Choi, N. B., Moreau, E., Berendt, A., and Mizeraczyk, J., "Trailing-Edge Separation Control of a NACA 0015 Airfoil Using Dielectric-Barrier-Discharge Plasma Actuators," *ERCOFTAC Bulletin*, Vol. 94, 2013, pp. 35–40.

[6] Moreau, E., "Airflow control by non-thermal plasma actuators," *Journal of Physics D: Applied Physics*, Vol. 40, No. 3, 2007, p. 605.

[7] Kronhaus, I., Eichler, S., and Schein, J., "Schlieren characterization of gas flows generated by cathodic arcs in atmospheric pressure environment," *Applied Physics Letters*, Vol. 104, No. 6, 2014, p. 063507.

[8] Kronhaus, I., Kuhn-Kauffeldt, M., and Schein, J., "Investigation of Cathodic Arc Plume in an Atmospheric Pressure Environment Using Stark Broadening," *Plasma Science, IEEE Transactions on*, Vol. 43, No. 10, 2015, pp. 3570–3575.

[9] Kronhaus, I. and Scharnowski, S., "Investigation of Cathodic-Arc-Jet Influence on Cross Flow using Particle Image Velocimetry," *46th AIAA Plasmadynamics and Lasers Conference*, 2015, p. 2806.

[10] Meunier, J.-L. and Drouet, M. G., "Experimental study of the effect of gas pressure on arc cathode erosion and redeposition in He, Ar, and SF6 from vacuum to atmospheric pressure," *Plasma Science, IEEE Transactions on*, Vol. 15, No. 5, 1987, pp. 515–519.

[11] Taylor, G., "The formation of a blast wave by a very intense explosion. I. Theoretical discussion," *Proceedings of the Royal Society of London. Series A, Mathematical and Physical Sciences*, 1950, pp. 159–174.

[12] Sedov, L. I., "Propagation of strong shock waves," *Journal of Applied Mathematics and Mechanics*, Vol. 10, 1946, pp. 241–250.

[13] Weller, H. G., Tabor, G., Jasak, H., and Fureby, C., "A tensorial approach to computational continuum mechanics using object-oriented techniques," *Computers in physics*, Vol. 12, No. 6, 1998, pp. 620–631.